ARC Geophysical Research

Chaotic Slow Slip Events in New Zealand from Two Coupled Slip Patches: A Proof of Concept

Thomas Poulet*[1], Sandro Truttmann[2], Victor Boussange[3,4], and Manolis Veveakis[5]

[1]CSIRO Mineral Resources, Perth, Australia
[2]Institute of Geological Sciences, University of Bern, Bern, Switzerland
[3]Swiss Federal Research Institute WSL, Birmensdorf, Switzerland
[4]Institute of Terrestrial Ecosystems, Department of Environmental System Science, ETH Zürich, Zürich, Switzerland
[5]Department of Civil and Environmental Engineering, Duke University, Durham, NC, USA

Abstract

Recent studies showed that seemingly random Slow Slip Events (SSEs) can display chaotic patterns within the largest source of seismic hazards in New Zealand, the Hikurangi subduction zone. Some irregular SSE occurrences are therefore not arbitrary but behave with short-term predictability. However, the forecasting challenge persists as observations remain too short and noisy to constrain purely data-driven solutions, calling for a physics-based modelling approach. Here we propose a physical model of two coupled oscillators, each capturing the behaviour of a single slow-slip patch, for the deep Kaimanawa and the shallow East Coast SSEs respectively. The simplified model successfully reproduces the type of chaotic behaviour observed at the Global Navigational Satellite System station in Gisborne, yielding SSEs of appropriately varying amplitude and duration. Those results reveal that the multi-physics response of the shear zone strongly controls the underlying system, even before accounting for any geometrical complexity or distribution of material properties.

Keywords: Slow Slip Events, Hikurangi Subduction Zone, Model Development, Multi-Physics, Coupled Oscillators

*Corresponding Author
E-mail address: thomas.poulet@csiro.au
doi:10.5149/ARC-GR.1579

1 Introduction

In subduction environments, frequently occurring Slow Slip Events (SSEs) significantly contribute to the overall deformation; they release large amounts of strain [16] and may even trigger large magnitude, destructive earthquakes [15, 32, 36, 47]. SSEs have been identified worldwide [59] through Global Navigation Satellite System (GNSS) monitoring [26] and their episodic behaviour seems universal. While some SSE systems reveal striking periodic recurrence intervals, e.g. in Cascadia [46], SSEs in New Zealand's Hikurangi subduction zone display much more irregular duration and recurrence times [56]. Interestingly, it was recently shown that SSEs can behave in a deterministic manner, not only in simpler geometrical environments like Cascadia [23] but also in New Zealand [52]. Those SSEs are therefore not random but chaotic, which means that both occurrence and magnitude could be described by a mathematical system of equations and that some short-term SSE predictability is theoretically possible. However, reliable forecasts are not yet available as monitoring observations have not been operating for long enough and remain too noisy for purely data-driven approaches [52].

Some physical understanding of shear zones is required, in general and in subduction environments specifically, to enhance the interpretation of observations. Fortunately, such knowledge progresses fast through theoretical [2, 45, 50], experimental [11, 25, 35], observational [13, 58], or numerical [43, 54] studies. However, no comprehensive model has yet been proposed to explain cases as complex as New Zealand and the challenge remains open to suggest an underlying system of equations controlling that system. Here, we present a first feasibility study.

2 Materials and Methods

2.1 The Oscillator Model

One multi-physics oscillator model [2] has shown its ability to explain single shear zone scenarios and link temporal evolution of subduction zones [54] with their corresponding spatial signature [40]. The system considers a fully saturated shear zone subject to shear heating and fluid release by chemical decomposition, with a rate- and temperature-dependent frictional behaviour in a low-permeability environment [51]. The shear zone, only meters thick [39, 40] but extending over kilometres, can be modelled in one dimension (1D) across its thickness as a function of temperature (T) and excess pore pressure (ΔP). While higher-dimensional models may offer additional insights into geometrical complexities [34], the 1D framework presents a powerful approach to identify and understand the core mechanisms driving localisation and episodic slip. In particular, the strong focus on the physics of processes makes it particularly suitable for testable predictions or falsifiable hypotheses. Shear heating from the creeping fault can eventually trigger reversible endothermic chemical reactions releasing fluid, capping the typical thermal runaway process [44], and whose extent can be tracked by the corresponding partial solid ratio (s). The resulting system of equations also includes the effects of the resulting pore pressurisation, porosity (ϕ) variation, and can be expressed as the evolution of two normalised state variables [54], the temperature (T) and excess pore pressure (ΔP), as functions of time (t) and space (z):

$$\begin{cases} \frac{\partial \Delta P}{\partial t} = \frac{\partial}{\partial z}\left[\frac{1}{Le}\frac{\partial \Delta P}{\partial z}\right] + (1-\phi)(1-s)\mu_r e^{\frac{Ar\delta T}{1+\delta T}} \\ \frac{\partial T}{\partial t} = \frac{\partial^2 T}{\partial z^2} + \left[Gr((1-\Delta P)_+)^n e^{\frac{\alpha Ar}{1+\delta T}} - (1-\phi)(1-s)\right] e^{\frac{Ar\delta T}{1+\delta T}} \end{cases} \tag{1}$$

where n denotes the rate sensitivity of friction and the subscript "+" the positive part of a term, to account for hydrofracturing cases. All dimensionless groups are defined in [2],

including two most important ones in this study, the Gruntfest (Gr) and Lewis (Le) numbers, as well as the three others (μ_r, Ar, and δ, not discussed here). The Gruntfest number [21], Gr, represents the ratio of mechanical work over the enthalpy of the chemical reaction, and the modified Lewis number, Le, is inversely proportional to permeability. The reduction of a complex system behaviour to the (spatial and temporal) evolution of temperature and fluid pressure highlights the importance of two of the main mechanisms involved: temperature increase by shear heating – which strongly affects the chemistry – and (low) permeability – which allows large fluid pressure build-ups that lubricate the fault core.

The model is one-dimensional across the shear zone given its finite thickness of a few meters [39], compared to the extension of the subduction zone in kilometres along its dip and hundreds of kilometres laterally. The values of all parameters determine the location (depth) of the oscillator.

From the resulting oscillator behaviour, we can retrieve the strain rate profile

$$\dot{\epsilon} = ((1 - \Delta P)_+)^n e^{\frac{-(1-\alpha)Ar}{1+\delta T}} \tag{2}$$

which can be integrated in space across the shear zone to obtain the velocity, and then integrated in time to get the displacement.

The system of Equations 1 is expressed in dimensionless form to highlight its controlling parameters. There exist various stability regimes [2] and for specific parameters the transient system exhibits a limit cycle leading to slip events lasting a few days – slow slip corresponding to observed seismic tremors – and occurring periodically every few months (Figure 1).

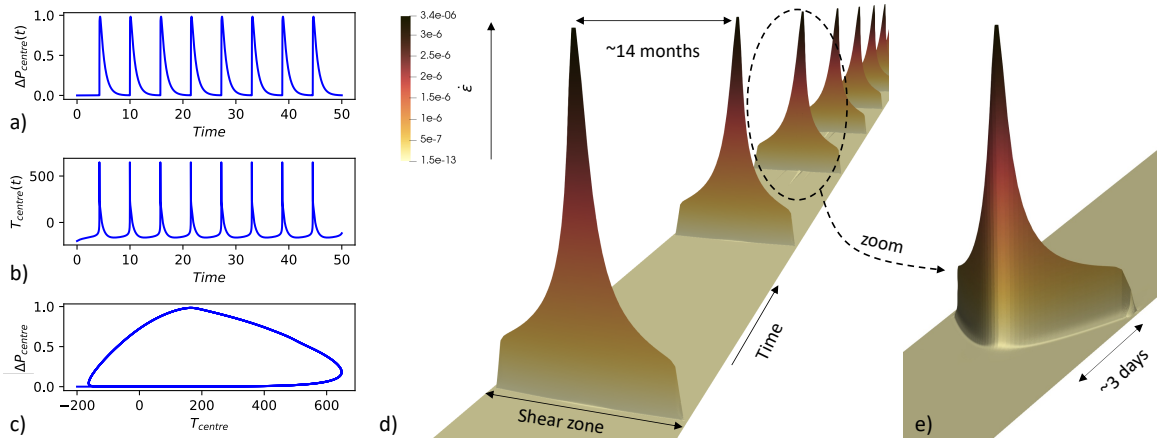

Figure 1: Response of a single multi-physics serpentinite oscillator modelling a one-dimensional (1D) chemical shear zone through a few stick–slip cycles. The model is based on two primary dimensionless variables: the temperature (T) and excess pore pressure (ΔP), following the system of Equations 1, with parameter values from Table 1 (Appendix A). Time evolution at the centre of the shear zone of (a) the normalised excess pore pressure ΔP_{centre}, with values between 0 and 1 indicating hydrostatic to lithostatic variations, and (b) the normalised temperature T_{centre}, with corresponding values ranging from 230°C to 453°C. (c) Plotting ΔP_{centre} versus T_{centre} shows the periodic limit cycle of the oscillator. (d) Profile evolution of strain rate $\dot{\epsilon}$, using Equation 2, showing strong localisation at the shear zone centre. Slip events occur every 14 months and last for a few days.

During each slip event, the temperature and fluid pressure increase dramatically at the centre of the shear zone (Figure 1a), highlighting the predominant roles of those properties on the response of the system. Such a single oscillator is applicable to scenarios with enough

geometrical simplicity for the 1D assumption to hold, like the Cascadia subduction zone [2], and can explain observed periodically recurring SSEs, called Episodic Tremor and Slip (ETS) events, occurring in a specific depth range [46]. The multi-physics (thermo-hydro-mechanical-chemical) nature of the system encompasses various behaviours including thermal dehydration [50], weakening [45], pressurisation of pore fluid [37], and healing [49]. The resulting oscillatory regime is confined to specific parameter ranges of the dimensionless parameters [3]. While previous analyses have mostly focused on the low permeability threshold below which oscillations occur [39], numerical analyses for specific parameter sets can establish quantitative bounds (e.g., Figure 5, Appendix A). The definition of these parameters offers a direct connection to physical properties, thereby enabling the prediction of specific depth ranges where SSEs can occur as a testable aspect of the model. This is one major advantage of using a physical model which enhances rate and state models [22], whose predictability cannot reach as far since their coefficients must be input by modellers.

2.2 New Zealand: Two Coupled Oscillators

In New Zealand, SSE patterns are much more complex and not as periodic as in Cascadia [56], likely related to the more heterogeneous structure of the Hikurangi subduction zone. Yet, these SSEs also exhibit characteristics of a chaotic system, raising hope for short-term predictability [52]. However, forecasts with purely data-driven methods require clean signals and long measurement periods, which are not available yet; this is where physics can help.

The curved geometry of the Hikurangi Trough off New Zealand marks the Southern end of the Kermadec and Tonga plates, which extend rather linearly over more than 2,000km northward (Figure 2b). Hence, we assume a 1D shear zone configuration away from the Southern end and focus on the northern-most SSEs in New Zealand, the Deep Kaimanawa SSEs and East Coast SSEs (Figure 2a) but ignore the Kapiti SSEs further South, since the 1D-assumption does not hold in the southern part of the Hikurangi subduction zone anymore due to its bending, adding further complexity [34]. SSEs might occur along the whole Kermadec and Tonga plate boundaries but cannot be detected since no offshore GNSS data is available. Based on cumulative slip observations [56], we consider a conceptual cross-section around Gisborne (Figure 2c) and interpret the presence of SSEs in two localised patches at different depth levels as two separate oscillator cells. For this conceptual analysis, we omit the question of rock composition in each patch and use a previously published oscillator based on carbonates for both oscillators [40] (Table 1, Appendix B). This choice leverages the flexibility of the dimensionless framework, which allows calibration for different geological settings. We do acknowledge the well-established lithologies, such as the smectite clay-rich volcaniclastic material in the shallow SSE region of northern Hikurangi, supported by IODP drilling [5, 49] and seismic imaging [19]. However, the self-similar nature of the mathematical system, characterised by an internal dimensionality of approximately 2.5 [54], permits adaptation to other compositions by tuning the Gruntfest and Lewis numbers for the same results. Therefore, the specific material used in this proof-of-concept study is not critical to the generality of the results. Similarly, the choice of a single material for the two distinct oscillators hides the specific signature of each behind the self-similarity of the mathematical system. Indeed, the Kaimanawa SSEs are much smaller and display less frequent large events than the East Coast SSEs [1]. This proof of concept uses different Gr and Le values to account for the differences in frequency and magnitude between the two oscillators [3] and does not include the difficult step of calibrating all parameters.

The physical focus of the model (Sec. 2.1) makes it particularly suitable to highlight its driving factors and allows for testable predictions, which we hope to see validated by laboratory experiments in the future. One notable limitation of this one-dimensional model,

however, is its restriction to perfectly periodic signals and subsequent inability to account for more complex geometrical complexity and less regular time evolution. This contribution addresses this specific limitation by coupling two oscillators to capture some geometrical interactions and explain the non-regular observations in time.

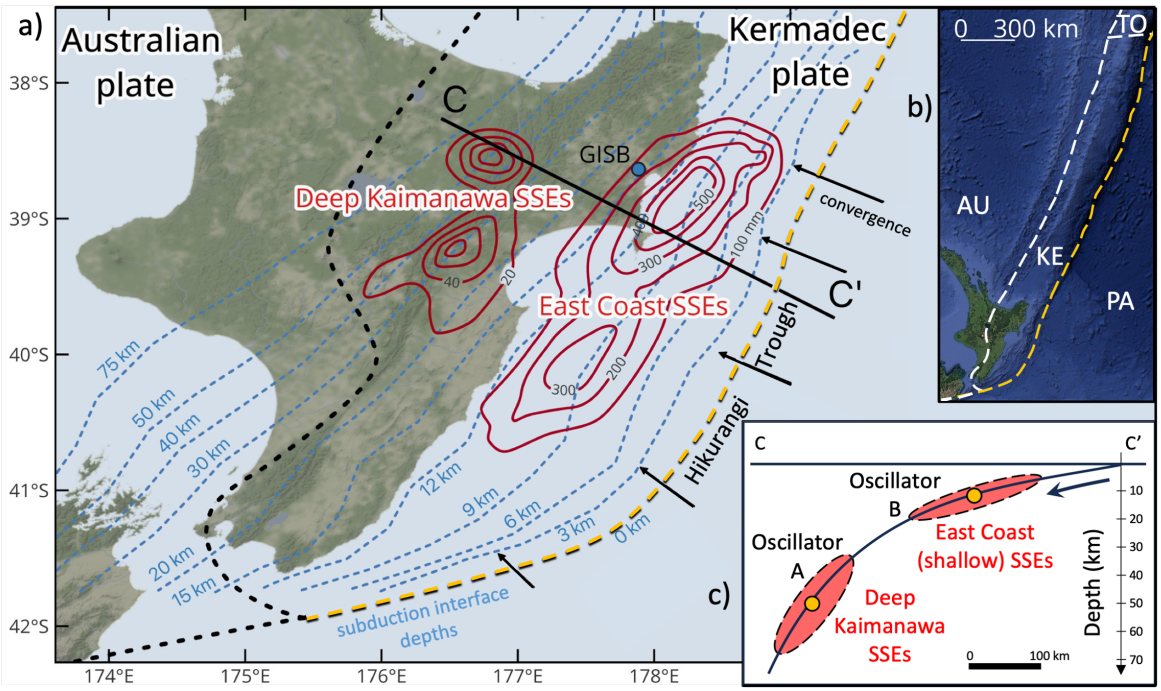

Figure 2: Selected Slow Slip Events in New Zealand's North Island. (a) Map showing cumulative slip contours (2002-2014) from the Deep Kaimanawa and East Coast SSEs as well as plate boundaries (black dashes), Hikurangi Trough (yellow dashes), subduction interface depths [56], and location of the Gisborne station (GISB, blue marker). (b) Larger scale view of the Kermadec (KE), Australian (AU), Pacific (PA) and Tonga (TO) plates, with plate boundaries (white dashes) and Hikurangi Trough (yellow dashes); The elongated profile of the Kermadec plate justifies ignoring geometry, at first order, on any subduction profile not too close to the plate's lower edge. c) Schematic vertical cross-section across the deep and shallow SSEs. Each slip patch is modelled by an oscillator.

The two oscillators correspond to slip patches at different depths for the same subduction zone and are geomechanically linked. Their exact interaction remains an open problem [57] but interactions between the deep and shallow part of a slab have been observed in subduction environments [18], with synchronisation between shallow and deep seismic activities [8, 28] pointing to the role of rigidity [48] among others. Here, we aim to demonstrate the potential of a physical approach to capture complex SSE patterns and model this SSE system by coupling the two oscillators, postulating that it is that coupling which controls its chaotic response [55]. Any slip event from one oscillator affects the other, mainly through the force chain along the connecting subduction zone. As the driving system arguably stems from greater depth and effects propagate upwards [39], we herein consider a one-way coupling only, where the slip events of the deep oscillator trigger excess forces on the shallower one, which can be simulated in a conceptual manner through the evolution of its Gruntfest number. This idealised coupling aims at identifying the responsible driving factor while avoiding the complex physical and geometrical considerations of the real configuration.

In that respect, we expect the two oscillators to communicate through the multiphysical

response of the connecting domain. This domain is, in principle, experiencing mechanical (velocity and displacement), thermal, and pore pressure gradients. In the present approach, all these fields are coupled (see Equation 2), thereby suggesting that linking the two oscillators could be performed directly through their boundary conditions, and in particular through the temperature field since excess pore pressure is equal to zero everywhere except inside the shear zones. As such, the simplest approach consists of coupling the two oscillators with a thermoelastic spring, assuming the two slip patches are connected in series and share the same stress $\sigma = E(\epsilon + \alpha\Delta T)$ through a thermoelastic connecting domain, where α denotes a thermal expansion coefficient and E an elastic modulus. The stress σ can then be calculated as $\sigma = (E_1 + E_2)\epsilon + (E_1\alpha_1\Delta T_1 + E_2\alpha_2\Delta T_2)$. This, in turn, means that stress perturbations under fixed displacement (constant strain) are driven by thermal stresses alone, which is a constraint of the current approach and should be generalised in the future. In the example of two Coulomb-type faults with friction coefficient μ, connected in series through a thermoelastic half-space under fixed displacement, the applied shear stress change would then be $\Delta\tau = \tau - \tau_0 = \mu\Delta\sigma = \mu(E_1\alpha_1\Delta T_1 + E_2\alpha_2\Delta T_2)$.

Based on these considerations, we take a proxy for the force transfer between connected oscillators through the evolution of the Gruntfest number [55], Gr. Since the strain rate is strongly temperature-controlled, we update Gr for one oscillator linearly with the temperature derivative of the other, as a proxy for slip events. Setting an activation value δT_{min} and a maximum bound δT_{max} for $\frac{\partial T_1}{\partial t}\Big|_{centre}$, we compute the proportionality coefficient as

$$\beta_1 = \left(\frac{\partial T_1}{\partial t}\Big|_{centre} - \delta T_{min} \right) / \left(\delta T_{max} - \delta T_{min} \right) \tag{3}$$

where δT_{min} and δT_{max} can be precomputed since the first (external/deep) oscillator is unperturbed (one-way coupling). The Gr parameter for the second (internal/shallow) oscillator can be expressed as

$$Gr_2 = Gr_{2_0} + \beta_1 \Delta Gr \tag{4}$$

where ΔGr is taken as a constant parameter, whose value is investigated in the study based on the resulting patterns obtained.

This approach allows to retrieve a variety of responses [27], including quasiperiodic dynamics when oscillators do not lock, entrainment with new period for small coupling strengths, period-doubling dynamics, and chaotic dynamics (Figure 3a). The high sensitivity of the parameters (e.g., Figure 3b) places the full picture of the various regimes beyond the scope of this study. We consider the displacement of the shallow oscillator as proxy observation to compare against GNSS data from the Gisborne station [20], which records the shallow East Coast SSEs exceptionally well (Figure 4a).

3 Results - Chaotic Displacement Patterns

The results show that we can recover a chaotic response of the system (Figure 3b), leading qualitatively to the displacement patterns observed, with instant slip events of various amplitudes and durations. By definition of a chaotic system, its response is fairly sensitive to input parameters and more periodic regimes can also be retrieved (Figure 3) as expected [27]. With the proof of concept established, we further investigate the parameter space. From a manual analysis, we show that other parameters allow to reproduce displacement results that are qualitatively close to real observations, with series of small temperature jumps interrupted by larger and longer jumps (Figure 4b). The comparison of the simulation results with observations remains conceptual, since the prototype nature of the one-way coupling used would

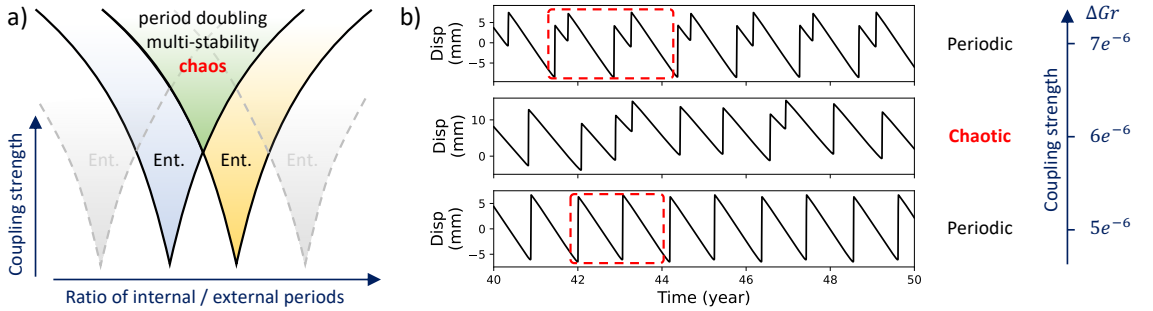

Figure 3: Possible responses of one-way coupling for two oscillators. (a) Schematic diagram illustrating the variety of responses possible [27], including quasi-periodicity when oscillators do not lock (outside coloured areas), entrainment regions ("Ent."), known as Arnold tongues [4], with new periods for small coupling strength, multi-stability, period-doubling, or chaotic dynamics for specific values of parameters. (b) Real example responses for our coupled oscillators, showing the sensitivity of the coupling strength and small parameter ranges leading to chaotic responses of fault slip at the shallow oscillator, with ΔGr defined in Equation 4. Red dashed windows indicate periodic patterns.

not warrant the considerable time required to calibrate such a complex and sensitive model. As such, only the temperature evolution is displayed (Figure 4b), to emphasise its role as the driving parameter responsible for the slip patterns, which would require extra parameter tuning to directly match observations.

4 Discussion

It is particularly exciting to use a physical system based on oscillators designed for single slip patches and retrieve signals that bear the characteristics of GNSS observations in more complex geometrical settings. Our approach ensures interpretability by using the minimum amount of complexity to obtain a chaotic response, with a one-way coupling between simplified one-dimensional oscillators which can only reproduce episodic events as perfectly periodic. We therefore argue that the oscillator model can not only explain the complex mechanisms at play, but also provide a potential tool to forecast irregular SSEs in New Zealand. Indeed, if the physical parameters can be calibrated to match observations, which falls beyond the scope of this study, then the phase space analysis [52] can be performed on the corresponding clean signal from the physical system, even with a two-way coupling, that could lead to the maximum theoretical predictions.

Despite the missing calibration step, we rebuild a multi-dimensional phase space of the results [12], which describes all possible states of the dynamical system, as was done from the GNSS data [52]. The resulting structure observed in phase space (Figure 4d) matches qualitatively that from GNSS observations (Figure 4c) and reveals the underlying attractor for those trajectories (Abarbanel, 1996). The critical difference is that we now have a description of the physical system involved. In particular, the presence of numerous cycles of smallest amplitude – corresponding to the inter-SSE signal [52] – indicate that there might be a stronger signal component than previously thought in those parts of the data usually thought of as noise, as previously proposed [17, 30, 31, 52]. This testable prediction also increases optimism for purely data-driven analyses and we are looking forward to learning, in time, whether it holds true or not as the quality of measurements and post-processing techniques increase the signal to noise ratios of observations.

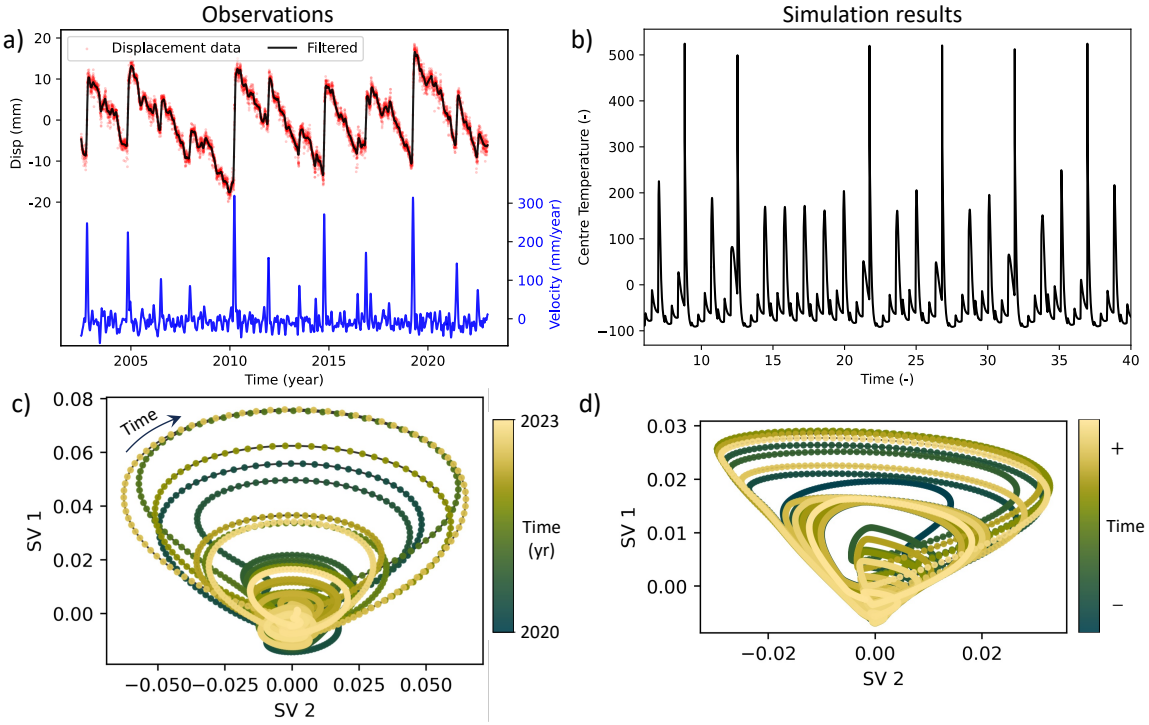

Figure 4: Qualitative comparison of observations from the GISB station (left) and the results of two coupled oscillators (right). (a) GNSS data from the GISB station, including daily positions (red dots), smoothed displacement (black) using low-pass Finite Impulse Response (FIR) filtering [52] (Appendix C) and corresponding slip velocity (blue). (b) Chaotic model results of dimensionless temperature evolution at the centre of the shear zone. (c) Phase space representation of the first two singular vectors (SV) derived by singular system analysis of GISB observations. Trajectories follow large cycles during SSEs and remain close to the origin in between (inter-SSE), whether as signal noise or small amplitude slip events. (d) Phase space representation of chaotic model results, displaying similar characteristics as for GISB observations. Here, the small inter-SSE cycles are not noise, given the noise-free simulation results.

In our case, the smallest jumps (Figure 4b) remain quasi-periodic because of the one-way coupling. Their occurrence could be perturbed by introducing the reciprocal coupling of the shallow oscillator impacting the deep one. This added complexity should be considered for realistic calibration attempts but goes beyond the scope of this study.

This study suggests the feasibility of using coupled slip oscillators to model New Zealand SSE characteristics, with potential applications to other SSEs globally, if several slip patches have been identified and a chaotic signal suspected. Amongst a growing trend of data-driven methods being deployed to analyse complex SSE observations [14, 23, 24, 29, 52], the complementarity of physics-based approaches remains key to identify controlling factors and explain the processes involved. The proposed oscillator model [54] can describe episodic SSEs, their timing (Figure 1d), duration (Figure 1e), spatial signature [40] and the underlying reason for the number and location of slip patches observed (Figure 2). Interestingly, it can also apply to one-off earthquakes [54] in similar environments, for which refined data processing reveals precursors with the same exponential build-up [7, 32]. With the oscillator model having previously shown its ability to capture and explain the behaviour of SSEs for a single slip patch, and the shallow New Zealand SSEs having been identified as the interaction between two

oscillators [Figure 7 of 39], this study proposes a model to capture that interaction, without introducing any geometrical complexity. The fact that an approximate one-way coupling of two oscillators can explain the chaotic behaviour and qualitatively match observations reinforces our suggestion that the physics of the shear zone really is the main control of the overall system behaviour, despite all the complexity not currently accounted for and which clearly plays a role, including 3D geometry and rheological heterogeneities of the subduction interface [38, 59]. This analysis helps balance the potentially excessive importance granted to geometrical factors [34].

This study highlights the effectiveness of simplified modelling, which should not suffer from our ability to simulate more realistic 3D problems. The homogenisation of an entire slip patch with a single oscillator aims at capturing the essence of the overall system instead of every aspect. The suggested prototype can and should eventually be extended with extra features for better applicability, including the continuous behaviour along the shear zone, 3D geometrical effects, two-way couplings, and more accurate non-instantaneous force coupling, including with other slip cells. Yet, the physical control of fluid-release reactions on complex SSEs at the large scale raises confidence that simplified underlying equations can be derived to simulate what is otherwise one of the most complex geological scenarios. Also, the analysis of the generated displacement signal in phase space (Figure 4d) highlights that small amplitude parts of observed signals are not necessarily noise or errors, which warns against too much smoothing on real-world SSE signals.

5 Conclusions

The characterisation of a complex subduction zone by the simple coupling of multi-physics oscillators demonstrates that complex SSE dynamics could be described by a physical system, implying exciting prospects in terms of SSE predictability. While nearly periodic SSE signals can intuitively be accepted as deterministic, like in Cascadia [23], it is fascinating to unravel the physical processes behind irregular signals from New Zealand equally identified as deterministic systems with chaotic dynamics [52]. Modelling the coupled force transfer interactions between two slip patches could explain chaotic SSEs in the Hikurangi subduction zone and potentially other settings, since various types of fault slip observations seem to arise from the same physical mechanisms [37]. Given the notable qualitative match between empirical data and the derived physical model, the latter could be calibrated with data-inference methods [9] to provide short-term predictions. Furthermore, the parameterization of dimensionless groups with a neural network could correct unresolved processes [6, 42], especially for the coupling, and additionally be used to improve our fundamental understanding of physical processes by an offline analysis of the learnt parametrization [41]. Alternatively, the physical processes that we have identified could be used to constrain data-driven approaches following a physics-informed neural network approach [33, 60], mitigating the problem of data deficiency. In either case, by harnessing physical knowledge of the underlying systems, these approaches could leverage the available data and greatly improve our capacity to forecast SSE and their fast, potentially destructive counterparts [16, 36, 53].

Acknowledgements

We thank Laura Wallace and the two anonymous reviewers for their thoughtful comments and constructive suggestions, which have greatly helped us improve the quality and clarity of this manuscript.

Code Availability

The code used to model the coupled oscillators is available [10] at https://zenodo.org/doi/10.5281/zenodo.13300509.

Data Availability

The GNSS data used in this study is available from GNS Science [20] at https://doi.org/10.21420/30F4-1A55.

Author Contributions

Conceptualisation, T.P. and M.V.
Methodology, T.P. and M.V.
Software, T.P., V.B. and S.T.
Visualisation, T.P.
Writing – Original Draft Preparation, T.P.
Writing – Review & Editing, M.V., V.B., S.T.

Appendix A Windows of Oscillations

The deceptively simple formulation of the idealised oscillator system (Equation 1) hides some complex responses of the model based on the values of all parameters [2]. The fault zone can indeed display three types of behaviours, either remaining in slow steady creep, experiencing a one-off slip event followed by faster steady creep, or following periodic stick-slip cycles. The system is sensitive to all parameters, with the Gruntfest number Gr and Lewis number Le playing major roles for specific chemical reaction [3]. Figure 5 shows ranges of (Gr, Le) values for which the deep oscillator results in periodic stick-slip events. This figure shows the permeability threshold above which oscillations stop (remembering the Lewis number is inversely proportional to permeability). Also, the bounded Gr values in Figure 5 and the dependency of the Gruntfest number with depth explain why SSE are only observed within specific depth windows.

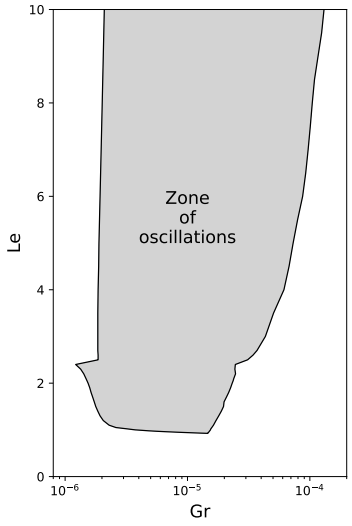

Figure 5: Zone of oscillations in Gr – Le space for the deep oscillator.

Appendix B Carbonate Oscillator Parameters for SSEs

To model the deep Kaimanawa SSEs and shallower East Coast SSEs, we use a carbonate oscillator with similar parameters (Table 1) to those published [40] for the Glarus Thrust in Switzerland. We refer the reader to the original study [2] for the definition of all parameters and corresponding explanations of the model. The material properties are indexed using subscripts A, B and AB, corresponding to a generic decomposition reaction

$$AB_{(s)} \rightleftharpoons A_{(s)} + B_{(f)} \tag{5}$$

where a solid AB decomposes into a solid A and a fluid B.

Table 1: Dimensionless model parameters and corresponding indicative material properties used for the deep Kaimanawa SSEs, based on published calcite oscillator [40].

Parameter	Value	Units
Dimensionless groups		
Gr	10^{-5}	–
Le	2.05	–
Ar	40	–
α	0.5	–
δ	10^{-3}	–
μ_r	10^{-3}	–
Material properties		
ΔE	104	kJ/mol
T_c	275	°C
K_c	7×10^8	–
ϕ_0	0.01	–
n	3	–
M_A	0.056	kg/mol
M_B	0.044	kg/mol
M_{AB}	0.1	kg/mol
ρ_A	3350	kg/mol
ρ_B	900	kg/mol
ρ_{AB}	2710	kg/mol

Appendix C Phase Space Reconstruction

Time series can conveniently be analysed using Singular Spectrum Analysis (Broomhead & King, 1986), which decomposes the trajectory matrix X, reconstructed from M lagged copies of the signal, into a sum of Singular Vectors (SV), similar to an eigenvalue decomposition. The SVs then represent the new coordinates in phase space, which is a frequently used nonlinear analysis tool to study system dynamics. In this study, we follow the approach detailed in a previous publication (Truttmann et al., 2024) and show 2D representations of resulting phase spaces (Figure 4), where the values of the first two vectors are used as coordinates, varying with time. For real observations (Figure 4c), raw data is herein smoothed by applying a low-pass finite impulse response (FIR) filter utilising a Hamming window, with a cut-off frequency of 1/50 and a window span of 60 days (Truttmann et al., 2024). Smooth data obtained from simulations can be transformed into phase space directly (Figure 4d). We then reconstruct the phase space coordinates using a window length of M = 60.

References

[1] F. Aden-Antoniów, W. B. Frank, C. J. Chamberlain, J. Townend, L. M. Wallace, and S. Bannister. Low-Frequency Earthquakes Downdip of Deep Slow Slip Beneath the North Island of New Zealand. *Journal of Geophysical Research: Solid Earth*, 129(5): e2023JB027971, May 2024. ISSN 2169-9313, 2169-9356. doi: 10.1029/2023JB027971. URL https://agupubs.onlinelibrary.wiley.com/doi/10.1029/2023JB027971.

[2] S. Alevizos, T. Poulet, and E. Veveakis. Thermo-poro-mechanics of chemically active creeping faults. 1: Theory and steady state considerations. *Journal of Geophysical Research: Solid Earth*, 119(6):4558–4582, June 2014. ISSN 2169-9313, 2169-9356. doi: 10.1002/2013JB010070. URL https://agupubs.onlinelibrary.wiley.com/doi/10.1002/2013JB010070.

[3] S. Alevizos, T. Poulet, M. Veveakis, and K. Regenauer-Lieb. Analysis of Dynamics in Multiphysics Modelling of Active Faults. *Mathematics*, 4(4):57, Sept. 2016. ISSN 2227-7390. doi: 10.3390/math4040057. URL https://www.mdpi.com/2227-7390/4/4/57.

[4] V. I. Arnol'd and A. Avez. *Ergodic problems of classical mechanics*. The Mathematical physics monograph series. Addison-Wesley, 1968.

[5] P. M. Barnes, L. M. Wallace, D. M. Saffer, R. E. Bell, M. B. Underwood, A. Fagereng, F. Meneghini, H. M. Savage, H. S. Rabinowitz, J. K. Morgan, H. Kitajima, S. Kutterolf, Y. Hashimoto, C. H. Engelmann De Oliveira, A. Noda, M. P. Crundwell, C. L. Shepherd, A. D. Woodhouse, R. N. Harris, M. Wang, S. Henrys, D. H. Barker, K. E. Petronotis, S. M. Bourlange, M. B. Clennell, A. E. Cook, B. E. Dugan, J. Elger, P. M. Fulton, D. Gamboa, A. Greve, S. Han, A. Hüpers, M. J. Ikari, Y. Ito, G. Y. Kim, H. Koge, H. Lee, X. Li, M. Luo, P. R. Malie, G. F. Moore, J. J. Mountjoy, D. D. McNamara, M. Paganoni, E. J. Screaton, U. Shankar, S. Shreedharan, E. A. Solomon, X. Wang, H.-Y. Wu, I. A. Pecher, L. J. LeVay, and IODP Expedition 372 Scientists. Slow slip source characterized by lithological and geometric heterogeneity. *Science Advances*, 6 (13):eaay3314, Mar. 2020. ISSN 2375-2548. doi: 10.1126/sciadv.aay3314. URL https://www.science.org/doi/10.1126/sciadv.aay3314.

[6] T. Beucler, P. Gentine, J. Yuval, A. Gupta, L. Peng, J. Lin, S. Yu, S. Rasp, F. Ahmed, P. A. O'Gorman, J. D. Neelin, N. J. Lutsko, and M. Pritchard. Climate-invariant machine learning. *Science Advances*, 10(6):eadj7250, Feb. 2024. ISSN 2375-2548. doi: 10.1126/sciadv.adj7250. URL https://www.science.org/doi/10.1126/sciadv.adj7250.

[7] M. Bouchon, V. Durand, D. Marsan, H. Karabulut, and J. Schmittbuhl. The long precursory phase of most large interplate earthquakes. *Nature Geoscience*, 6(4):299–302, Apr. 2013. ISSN 1752-0894, 1752-0908. doi: 10.1038/ngeo1770. URL https://www.nature.com/articles/ngeo1770.

[8] M. Bouchon, A. Socquet, D. Marsan, S. Guillot, V. Durand, B. Gardonio, M. Campillo, H. Perfettini, J. Schmittbuhl, F. Renard, and A.-M. Boullier. Observation of rapid long-range seismic bursts in the Japan Trench subduction leading to the nucleation of the Tohoku earthquake. *Earth and Planetary Science Letters*, 594:117696, Sept. 2022. ISSN 0012821X. doi: 10.1016/j.epsl.2022.117696. URL https://linkinghub.elsevier.com/retrieve/pii/S0012821X22003326.

[9] V. Boussange, P. V. Aceituno, F. Schäfer, and L. Pellissier. Partitioning time series to improve process-based models with machine learning, July 2022. URL http://biorxiv.org/lookup/doi/10.1101/2022.07.25.501365.

[10] V. Boussange, T. Poulet, and S. Truttmann. vboussange/coupledOscillators: v0.0.1, Aug. 2024. URL https://zenodo.org/doi/10.5281/zenodo.13300509.

[11] N. Brantut, A. Schubnel, J. Rouzaud, F. Brunet, and T. Shimamoto. High-velocity frictional properties of a clay-bearing fault gouge and implications for earthquake mechanics. *Journal of Geophysical Research: Solid Earth*, 113(B10):2007JB005551, Oct. 2008. ISSN 0148-0227. doi: 10.1029/2007JB005551. URL https://agupubs.onlinelibrary.wiley.com/doi/10.1029/2007JB005551.

[12] D. Broomhead and G. P. King. Extracting qualitative dynamics from experimental data. *Physica D: Nonlinear Phenomena*, 20(2-3):217–236, June 1986. ISSN 01672789. doi: 10.1016/0167-2789(86)90031-X. URL https://linkinghub.elsevier.com/retrieve/pii/016727898690031X.

[13] C. Collettini, C. Viti, T. Tesei, and S. Mollo. Thermal decomposition along natural carbonate faults during earthquakes. *Geology*, 41(8):927–930, Aug. 2013. ISSN 1943-2682, 0091-7613. doi: 10.1130/G34421.1. URL http://pubs.geoscienceworld.org/geology/article/41/8/927/131363/Thermal-decomposition-along-natural-carbonate.

[14] F. Corbi, J. Bedford, L. Sandri, F. Funiciello, A. Gualandi, and M. Rosenau. Predicting Imminence of Analog Megathrust Earthquakes With Machine Learning: Implications for Monitoring Subduction Zones. *Geophysical Research Letters*, 47(7):e2019GL086615, Apr. 2020. ISSN 0094-8276, 1944-8007. doi: 10.1029/2019GL086615. URL https://agupubs.onlinelibrary.wiley.com/doi/10.1029/2019GL086615.

[15] K. Dascher-Cousineau and R. Bürgmann. Global subduction slow slip events and associated earthquakes. *Science Advances*, 10(35):eado2191, Aug. 2024. ISSN 2375-2548. doi: 10.1126/sciadv.ado2191. URL https://www.science.org/doi/10.1126/sciadv.ado2191.

[16] T. H. Dixon, Y. Jiang, R. Malservisi, R. McCaffrey, N. Voss, M. Protti, and V. Gonzalez. Earthquake and tsunami forecasts: Relation of slow slip events to subsequent earthquake rupture. *Proceedings of the National Academy of Sciences*, 111(48):17039–17044, Dec. 2014. ISSN 0027-8424, 1091-6490. doi: 10.1073/pnas.1412299111. URL https://pnas.org/doi/full/10.1073/pnas.1412299111.

[17] W. B. Frank. Slow slip hidden in the noise: The intermittence of tectonic release. *Geophysical Research Letters*, 43(19), Oct. 2016. ISSN 0094-8276, 1944-8007. doi: 10.1002/2016GL069537. URL https://agupubs.onlinelibrary.wiley.com/doi/10.1002/2016GL069537.

[18] B. Gardonio, D. Marsan, T. Bodin, A. Socquet, S. Durand, M. Radiguet, Y. Ricard, and A. Schubnel. Change of deep subduction seismicity after a large megathrust earthquake. *Nature Communications*, 15(1):60, Jan. 2024. ISSN 2041-1723. doi: 10.1038/s41467-023-43935-3. URL https://www.nature.com/articles/s41467-023-43935-3.

[19] A. C. Gase, N. L. Bangs, D. M. Saffer, S. Han, P. K. Miller, R. E. Bell, R. Arai, S. A. Henrys, S. Kodaira, R. Davy, L. Frahm, and D. H. Barker. Subducting volcaniclastic-rich upper crust supplies fluids for shallow megathrust and slow slip. *Science Advances*, 9(33):eadh0150, Aug. 2023. ISSN 2375-2548. doi: 10.1126/sciadv.adh0150. URL https://www.science.org/doi/10.1126/sciadv.adh0150.

[20] GNS Science. GeoNet Aotearoa New Zealand Continuous GNSS Network - Time Series Dataset, 2000. URL https://data.gns.cri.nz/metadata/srv/eng/catalog.search#/metadata/feada279-c87d-4455-84c3-5eec115d617b.

[21] I. J. Gruntfest. Thermal Feedback in Liquid Flow; Plane Shear at Constant Stress. *Transactions of the Society of Rheology*, 7(1):195–207, Mar. 1963. ISSN 0038-0032. doi: 10.1122/1.548954. URL https://pubs.aip.org/jor/article/7/1/195/417821/Thermal-Feedback-in-Liquid-Flow-Plane-Shear-at.

[22] J.-C. Gu, J. R. Rice, A. L. Ruina, and S. T. Tse. Slip motion and stability of a single degree of freedom elastic system with rate and state dependent friction. *Journal of the Mechanics and Physics of Solids*, 32(3):167–196, Jan. 1984. ISSN 00225096. doi: 10.1016/0022-5096(84)90007-3. URL https://linkinghub.elsevier.com/retrieve/pii/0022509684900073.

[23] A. Gualandi, J.-P. Avouac, S. Michel, and D. Faranda. The predictable chaos of slow earthquakes. *Science Advances*, 6(27):eaaz5548, July 2020. ISSN 2375-2548. doi: 10.1126/sciadv.aaz5548. URL https://www.science.org/doi/10.1126/sciadv.aaz5548.

[24] A. Gualandi, L. Dal Zilio, D. Faranda, and G. Mengaldo. Similarities and Differences Between Natural and Simulated Slow Earthquakes. *Geophysical Research Letters*, 51(14):e2024GL109845, July 2024. ISSN 0094-8276, 1944-8007. doi: 10.1029/2024GL109845. URL https://agupubs.onlinelibrary.wiley.com/doi/10.1029/2024GL109845.

[25] R. Han, T. Shimamoto, T. Hirose, J.-H. Ree, and J.-i. Ando. Ultralow Friction of Carbonate Faults Caused by Thermal Decomposition. *Science*, 316(5826):878–881, May 2007. ISSN 0036-8075, 1095-9203. doi: 10.1126/science.1139763. URL https://www.science.org/doi/10.1126/science.1139763.

[26] M. Heflin, A. Donnellan, J. Parker, G. Lyzenga, A. Moore, L. G. Ludwig, J. Rundle, J. Wang, and M. Pierce. Automated Estimation and Tools to Extract Positions, Velocities, Breaks, and Seasonal Terms From Daily GNSS Measurements: Illuminating Nonlinear Salton Trough Deformation. *Earth and Space Science*, 7(7):e2019EA000644, 2020. ISSN 2333-5084. doi: 10.1029/2019EA000644. URL https://onlinelibrary.wiley.com/doi/abs/10.1029/2019EA000644. _eprint: https://agupubs.onlinelibrary.wiley.com/doi/pdf/10.1029/2019EA000644.

[27] M. L. Heltberg, S. Krishna, L. P. Kadanoff, and M. H. Jensen. A tale of two rhythms: Locked clocks and chaos in biology. *Cell Systems*, 12(4):291–303, Apr. 2021. ISSN 24054712. doi: 10.1016/j.cels.2021.03.003. URL https://linkinghub.elsevier.com/retrieve/pii/S2405471221001083.

[28] J. Jara, A. Socquet, D. Marsan, and M. Bouchon. Long-Term Interactions Between Intermediate Depth and Shallow Seismicity in North Chile Subduction Zone. *Geophysical Research Letters*, 44(18):9283–9292, Sept. 2017. ISSN 0094-8276, 1944-8007. doi: 10.1002/2017GL075029. URL https://agupubs.onlinelibrary.wiley.com/doi/10.1002/2017GL075029.

[29] C. W. Johnson and P. A. Johnson. Seismic Features Predict Ground Motions During Repeating Caldera Collapse Sequence. *Geophysical Research Letters*, 51(11):e2024GL108288, June 2024. ISSN 0094-8276, 1944-8007. doi: 10.1029/2024GL108288. URL https://agupubs.onlinelibrary.wiley.com/doi/10.1029/2024GL108288.

[30] R. Jolivet and W. B. Frank. The Transient and Intermittent Nature of Slow Slip. *AGU Advances*, 1(1):e2019AV000126, Mar. 2020. ISSN 2576-604X, 2576-604X. doi: 10.1029/2019AV000126. URL https://agupubs.onlinelibrary.wiley.com/doi/10.1029/2019AV000126.

[31] A. Kato and S. Nakagawa. Detection of deep low-frequency earthquakes in the Nankai subduction zone over 11 years using a matched filter technique. *Earth, Planets and Space*, 72(1):128, Dec. 2020. ISSN 1880-5981. doi: 10.1186/s40623-020-01257-4. URL https://earth-planets-space.springeropen.com/articles/10.1186/s40623-020-01257-4.

[32] A. Kato, K. Obara, T. Igarashi, H. Tsuruoka, S. Nakagawa, and N. Hirata. Propagation of Slow Slip Leading Up to the 2011 M_{w} 9.0 Tohoku-Oki Earthquake. *Science*, 335 (6069):705–708, Feb. 2012. ISSN 0036-8075, 1095-9203. doi: 10.1126/science.1215141. URL https://www.science.org/doi/10.1126/science.1215141.

[33] J. H. Lagergren, J. T. Nardini, R. E. Baker, M. J. Simpson, and K. B. Flores. Biologically-informed neural networks guide mechanistic modeling from sparse experimental data. *PLOS Computational Biology*, 16(12):e1008462, Dec. 2020. ISSN 1553-7358. doi: 10.1371/journal.pcbi.1008462. URL https://dx.plos.org/10.1371/journal.pcbi.1008462.

[34] J. Lee, V. C. Tsai, G. Hirth, A. Chatterjee, and D. T. Trugman. Fault-network geometry influences earthquake frictional behaviour. *Nature*, June 2024. ISSN 0028-0836, 1476-4687. doi: 10.1038/s41586-024-07518-6. URL https://www.nature.com/articles/s41586-024-07518-6.

[35] C. Marone. Laboratory-derived friction laws and their application to seismic faulting. *Annual Review of Earth and Planetary Sciences*, 26(1):643–696, May 1998. ISSN 0084-6597, 1545-4495. doi: 10.1146/annurev.earth.26.1.643. URL https://www.annualreviews.org/doi/10.1146/annurev.earth.26.1.643.

[36] K. Obara and A. Kato. Connecting slow earthquakes to huge earthquakes. *Science*, 353 (6296):253–257, July 2016. ISSN 0036-8075, 1095-9203. doi: 10.1126/science.aaf1512. URL https://www.science.org/doi/10.1126/science.aaf1512.

[37] F. X. Passelègue, M. Almakari, P. Dublanchet, F. Barras, J. Fortin, and M. Violay. Initial effective stress controls the nature of earthquakes. *Nature Communications*, 11 (1):5132, Oct. 2020. ISSN 2041-1723. doi: 10.1038/s41467-020-18937-0. URL https://www.nature.com/articles/s41467-020-18937-0.

[38] A. Perez-Silva, Y. Kaneko, M. Savage, L. Wallace, D. Li, and C. Williams. Segmentation of Shallow Slow Slip Events at the Hikurangi Subduction Zone Explained by Along-Strike Changes in Fault Geometry and Plate Convergence Rates. *Journal of Geophysical Research: Solid Earth*, 127(1):e2021JB022913, Jan. 2022. ISSN 2169-9313, 2169-9356. doi: 10.1029/2021JB022913. URL https://agupubs.onlinelibrary.wiley.com/doi/10.1029/2021JB022913.

[39] T. Poulet, E. Veveakis, K. Regenauer-Lieb, and D. A. Yuen. Thermo-poro-mechanics of chemically active creeping faults: 3. The role of serpentinite in episodic tremor and slip sequences, and transition to chaos. *Journal of Geophysical Research: Solid Earth*, 119(6):4606–4625, June 2014. ISSN 2169-9313, 2169-9356. doi: 10.1002/2014JB011004. URL https://agupubs.onlinelibrary.wiley.com/doi/10.1002/2014JB011004.

[40] T. Poulet, M. Veveakis, M. Herwegh, T. Buckingham, and K. Regenauer-Lieb. Modeling episodic fluid-release events in the ductile carbonates of the Glarus thrust. *Geophysical Research Letters*, 41(20):7121–7128, Oct. 2014. ISSN 0094-8276, 1944-8007. doi: 10.1002/2014GL061715. URL https://agupubs.onlinelibrary.wiley.com/doi/10.1002/2014GL061715.

[41] C. Rackauckas, Y. Ma, J. Martensen, C. Warner, K. Zubov, R. Supekar, D. Skinner, A. Ramadhan, and A. Edelman. Universal Differential Equations for Scientific Machine Learning, 2020. URL https://arxiv.org/abs/2001.04385. Version Number: 4.

[42] S. Rasp, M. S. Pritchard, and P. Gentine. Deep learning to represent subgrid processes in climate models. *Proceedings of the National Academy of Sciences*, 115(39):9684–9689, Sept. 2018. ISSN 0027-8424, 1091-6490. doi: 10.1073/pnas.1810286115. URL https://pnas.org/doi/full/10.1073/pnas.1810286115.

[43] H. Rattez, I. Stefanou, J. Sulem, M. Veveakis, and T. Poulet. The importance of Thermo-Hydro-Mechanical couplings and microstructure to strain localization in 3D continua with application to seismic faults. Part II: Numerical implementation and post-bifurcation analysis. *Journal of the Mechanics and Physics of Solids*, 115:1–29, June 2018. ISSN 00225096. doi: 10.1016/j.jmps.2018.03.003. URL https://linkinghub.elsevier.com/retrieve/pii/S0022509617309638.

[44] K. Regenauer-Lieb and D. A. Yuen. Rapid conversion of elastic energy into plastic shear heating during incipient necking of the lithosphere. *Geophysical Research Letters*, 25 (14):2737–2740, July 1998. ISSN 0094-8276, 1944-8007. doi: 10.1029/98GL02056. URL https://agupubs.onlinelibrary.wiley.com/doi/10.1029/98GL02056.

[45] J. R. Rice. Heating and weakening of faults during earthquake slip. *Journal of Geophysical Research: Solid Earth*, 111(B5):2005JB004006, May 2006. ISSN 0148-0227. doi: 10.1029/2005JB004006. URL https://agupubs.onlinelibrary.wiley.com/doi/10.1029/2005JB004006.

[46] G. Rogers and H. Dragert. Episodic Tremor and Slip on the Cascadia Subduction Zone: The Chatter of Silent Slip. *Science*, 300(5627):1942–1943, June 2003. ISSN 0036-8075, 1095-9203. doi: 10.1126/science.1084783. URL https://www.science.org/doi/10.1126/science.1084783.

[47] S. Ruiz, M. Metois, A. Fuenzalida, J. Ruiz, F. Leyton, R. Grandin, C. Vigny, R. Madariaga, and J. Campos. Intense foreshocks and a slow slip event preceded the 2014 Iquique M_w 8.1 earthquake. *Science*, 345(6201):1165–1169, Sept. 2014. ISSN 0036-8075, 1095-9203. doi: 10.1126/science.1256074. URL https://www.science.org/doi/10.1126/science.1256074.

[48] V. Sallarès and C. R. Ranero. Upper-plate rigidity determines depth-varying rupture behaviour of megathrust earthquakes. *Nature*, 576(7785):96–101, Dec. 2019. ISSN 0028-0836, 1476-4687. doi: 10.1038/s41586-019-1784-0. URL https://www.nature.com/articles/s41586-019-1784-0.

[49] S. Shreedharan, D. Saffer, L. M. Wallace, and C. Williams. Ultralow frictional healing explains recurring slow slip events. *Science*, 379(6633):712–717, Feb. 2023. ISSN 0036-8075, 1095-9203. doi: 10.1126/science.adf4930. URL https://www.science.org/doi/10.1126/science.adf4930.

[50] J. Sulem and V. Famin. Thermal decomposition of carbonates in fault zones: Slip-weakening and temperature-limiting effects. *Journal of Geophysical Research: Solid Earth*, 114(B3):2008JB006004, Mar. 2009. ISSN 0148-0227. doi: 10.1029/2008JB006004. URL https://agupubs.onlinelibrary.wiley.com/doi/10.1029/2008JB006004.

[51] N. Tisato, C. D. Bland, H. Van Avendonk, N. Bangs, H. Garza, O. Alamoudi, K. Olsen, and A. Gase. Permeability and Elastic Properties of Rocks From the Northern Hikurangi Margin: Implications for Slow-Slip Events. *Geophysical Research Letters*, 51(2): e2023GL103696, Jan. 2024. ISSN 0094-8276, 1944-8007. doi: 10.1029/2023GL103696. URL https://agupubs.onlinelibrary.wiley.com/doi/10.1029/2023GL103696.

[52] S. Truttmann, T. Poulet, L. Wallace, M. Herwegh, and M. Veveakis. Slow Slip Events in New Zealand: Irregular, yet Predictable? *Geophysical Research Letters*, 51(6): e2023GL107741, Mar. 2024. ISSN 0094-8276, 1944-8007. doi: 10.1029/2023GL107741. URL https://agupubs.onlinelibrary.wiley.com/doi/10.1029/2023GL107741.

[53] N. Uchida, T. Iinuma, R. M. Nadeau, R. Bürgmann, and R. Hino. Periodic slow slip triggers megathrust zone earthquakes in northeastern Japan. *Science*, 351(6272):488–492, Jan. 2016. ISSN 0036-8075, 1095-9203. doi: 10.1126/science.aad3108. URL https://www.science.org/doi/10.1126/science.aad3108.

[54] E. Veveakis, T. Poulet, and S. Alevizos. Thermo-poro-mechanics of chemically active creeping faults: 2. Transient considerations. *Journal of Geophysical Research: Solid Earth*, 119(6):4583–4605, June 2014. ISSN 2169-9313, 2169-9356. doi: 10.1002/2013JB010071. URL https://agupubs.onlinelibrary.wiley.com/doi/10.1002/2013JB010071.

[55] E. Veveakis, S. Alevizos, and T. Poulet. Episodic Tremor and Slip (ETS) as a chaotic multiphysics spring. *Physics of the Earth and Planetary Interiors*, 264:20–34, Mar. 2017. ISSN 00319201. doi: 10.1016/j.pepi.2016.10.002. URL https://linkinghub.elsevier.com/retrieve/pii/S0031920116302230.

[56] L. M. Wallace. Slow Slip Events in New Zealand. *Annual Review of Earth and Planetary Sciences*, 48(1):175–203, May 2020. ISSN 0084-6597, 1545-4495. doi: 10.1146/annurev-earth-071719-055104. URL https://www.annualreviews.org/doi/10.1146/annurev-earth-071719-055104.

[57] L. M. Wallace, J. Beavan, S. Bannister, and C. Williams. Simultaneous long-term and short-term slow slip events at the Hikurangi subduction margin, New Zealand: Implications for processes that control slow slip event occurrence, duration, and migration. *Journal of Geophysical Research: Solid Earth*, 117(B11):2012JB009489, Nov. 2012. ISSN 0148-0227. doi: 10.1029/2012JB009489. URL https://agupubs.onlinelibrary.wiley.com/doi/10.1029/2012JB009489.

[58] E. Warren-Smith, B. Fry, L. Wallace, E. Chon, S. Henrys, A. Sheehan, K. Mochizuki, S. Schwartz, S. Webb, and S. Lebedev. Episodic stress and fluid pressure cycling in subducting oceanic crust during slow slip. *Nature Geoscience*, 12(6):475–481, June 2019. ISSN 1752-0894, 1752-0908. doi: 10.1038/s41561-019-0367-x. URL https://www.nature.com/articles/s41561-019-0367-x.

[59] H. Weng and J.-P. Ampuero. Integrated rupture mechanics for slow slip events and earthquakes. *Nature Communications*, 13(1):7327, Nov. 2022. ISSN 2041-1723. doi: 10.1038/s41467-022-34927-w. URL https://www.nature.com/articles/s41467-022-34927-w.

[60] A. Yazdani, L. Lu, M. Raissi, and G. E. Karniadakis. Systems biology informed deep learning for inferring parameters and hidden dynamics. *PLOS Computational Biology*, 16(11):e1007575, Nov. 2020. ISSN 1553-7358. doi: 10.1371/journal.pcbi.1007575. URL https://dx.plos.org/10.1371/journal.pcbi.1007575.